

UV completion of 2D Ising CFT: a golden E_8 massless S -matrix

Changrim Ahn[†] and Minkyoo Kim^{‡,b}

[†]*Department of Physics, Ewha Womans University, Seoul 03760, Korea*

[‡]*RIBS & Department of Physics and Astronomy, Seoul National University, Seoul 08826, Korea*

^b*School of Science, Huzhou Normal University, Huzhou 313000, China*

We present a full classification of UV complete QFTs that RG flow to the 2D Ising CFT by solving the bootstrap equations for massless right–left S -matrices. For the Ising model with E_8 spectrum we find exactly four completions, arising from higher- $T\bar{T}$ -type deformations, including a previously unknown “golden flow” whose UV fixed point is a diagonal $su(2)$ coset CFT ($c = 25/14$) along $\Delta_{\text{rel}} = 2/7$. A universal Fibonacci/ E_8 structure governs the R–L adjacency matrices and the Y -system periods, so that the E_8 symmetry persists across all RG scales.

I. INTRODUCTION

The two-dimensional (2D) Ising conformal field theory (CFT) is one of the most fundamental building blocks of string theories as well as many other applications. Our prime goal is to find a complete list of UV CFTs and deformations which RG flow into the 2D Ising CFT in terms of concrete S -matrices based on the integrability. For this purpose, we need to find all exact S -matrices which can describe the Ising CFT in the IR limit and irrelevant deformations.

A systematic approach was proposed in [1] where the RG flows are constructed by S -matrices between massless particles describing the IR theory. In the massless limit, the excitations split into right (R) and left (L) movers. The right–right (R–R) and left–left (L–L) S -matrix amplitudes are the same as those of the massively deformed IR CFT. Deforming an integrable field theory by the irrelevant fields built from the higher $T\bar{T}$ -type conserved charges generates CDD-like scalar factors in the massive S -matrices [2, 3]. These factors contribute the right–left (R–L) and left–right (L–R) S -matrices in the massless limit [1]. Thermodynamic Bethe ansatz (TBA) equations derived from these amplitudes identify UV complete theories connected to the IR CFT by the RG flows.

The 2D Ising CFT can maintain integrability upon two particular deformations. Deformed by the energy operator, this is described by a massive free Majorana fermion. Using this simple S -matrix, one can still compute various interesting correlation functions. The other deformation is obtained by the magnetic spin operator. This integrable field theory is given by the Zamolodchikov’s celebrated S -matrix with eight self-conjugate particles, whose masses are given by the Perron-Frobenius eigenvector of the E_8 symmetry [4]. Some of these excitations have been experimentally observed with a golden mass ratio $m_2/m_1 = 2 \cos(\pi/5) = \varphi$ [5].

The Ising CFT is thus described by *two* distinct massless theories, the free-fermion one and the E_8 one, recovered as the massless (conformal) limits of the two massive deformations. For the free-fermion one with the (R–R) and (L–L) S -matrices -1 , the R–L S -matrices that generate RG flows into the tricritical Ising CFT with

$c = 7/10$ [6] or $N=1$ supersymmetric CFTs with $c = 3/2$ [7, 8] have been previously found.

Our main interest is to represent the Ising CFT as a scattering theory of the eight particles in the massless limit $m_1 \rightarrow 0$ while maintaining the mass ratios m_a/m_1 , which are proportional to the E_8 Perron-Frobenius eigenvector elements. While the (R–R) and (L–L) amplitudes are the same as Zamolodchikov’s S -matrix, explicit expressions of the (R–L) and (L–R) S -matrices have been missing. Although a previous study found three UV completions—diagonal, minimal, and saturated—without explicit S -matrices, complete analysis of the RG flows is not available [1]. For the minimal case, a conjectured TBA proposed in [9] remains unproven. Our result in this letter provides not only explicit S -matrices and TBAs for these three cases but also discovers one additional UV completion, the “golden”. We also find a universal relation based on the E_8 symmetry that connects all these four.

For a full classification, we need to find complete solutions of the massless bootstrap equations which have been used in A_n scattering theories [10]. As a summary, we (i) construct the finite positive R–L amplitudes satisfying the bootstrap and saturation bound which generate not only the three UV completions but also the new “golden” solution; (ii) derive its TBA/ Y -system by inversion relations and read off the UV central charge and the relevant deforming field; (iii) identify the golden UV candidate as the diagonal coset $(su(2)_5 \times su(2)_5)/su(2)_{10}$ from this TBA data and its $\Delta = 2/7$ operator content, checked against the genuine affine-branching spectrum; and (iv) check the relevant massless Y -system periods by exact integer/tropical Y -pattern computations.

II. NEW SOLUTIONS OF THE BOOTSTRAP

The elementary CDD block can be expressed with

$$F_p(\theta) \equiv \frac{\sinh \theta - i \sin(\pi p/30)}{\sinh \theta + i \sin(\pi p/30)}, \quad p \in \mathbb{Z}. \quad (1)$$

Each block is crossing-unitary, $F_p(\theta)F_p(\theta + i\pi) = 1$, and pole-free in the physical strip. Using $F_{30-p} = F_p$,

TABLE I. Complete R–L amplitude tables of the minimal and golden completions ($a \leq b$, $S_{ba} = S_{ab}$), $S_{ab} = \prod_p [p]^{n_{ab}(p)}$ with the shorthand $[p] \equiv F_p(\theta)$ for compactness. The exponents define the matrices $n(p)$ used below.

	minimal	golden		minimal	golden
S_{11}	[1][11]	[7][13]	S_{36}	[5][7] ² [9][11][13] ² [15]	[1][3][5][7] ² [9] ² [11] ³ [13] ³ [15]
S_{12}	[7][13]	[1][7][11][13]	S_{37}	[3][5][7][9] ² [11] ² [13] ² [15]	[3][5] ² [7] ² [9] ³ [11] ³ [13] ³ [15] ²
S_{13}	[2][10][12]	[6][8][12][14]	S_{38}	[4][6] ² [8] ² [10] ² [12] ² [14] ³	[2][4] ² [6] ² [8] ³ [10] ⁴ [12] ⁴ [14] ⁴
S_{14}	[6][10][14]	[4][8][10][12][14]	S_{44}	[1][5][7][9][11] ² [13][15]	[3][5][7] ² [9] ² [11] ² [13] ³ [15]
S_{15}	[3][9][11][13]	[5][7][9][11][13][15]	S_{45}	[4][6][8] ² [10][12] ² [14] ²	[2][4][6] ² [8] ² [10] ³ [12] ³ [14] ³
S_{16}	[6][8][12][14]	[2][6][8][10][12] ² [14]	S_{46}	[3][5][7][9] ² [11] ² [13] ² [15]	[3][5] ² [7] ² [9] ³ [11] ³ [13] ³ [15] ²
S_{17}	[4][8][10][12][14]	[4][6][8][10] ² [12][14] ²	S_{47}	[3][5][7] ² [9] ² [11] ² [13] ³ [15]	[1][3][5] ² [7] ³ [9] ³ [11] ⁴ [13] ⁴ [15] ²
S_{18}	[5][7][9][11][13][15]	[3][5][7][9] ² [11] ² [13] ² [15]	S_{48}	[2][4][6] ² [8] ² [10] ³ [12] ³ [14] ³	[2][4] ² [6] ³ [8] ⁴ [10] ⁴ [12] ⁵ [14] ⁵
S_{22}	[1][7][11][13]	[1][7] ² [11][13] ²	S_{55}	[1][3][5][7][9] ² [11] ³ [13] ² [15]	[3][5] ² [7] ³ [9] ³ [11] ³ [13] ⁴ [15] ²
S_{23}	[6][8][12][14]	[2][6][8][10][12] ² [14]	S_{56}	[4][6] ² [8] ² [10] ² [12] ² [14] ³	[2][4] ² [6] ² [8] ³ [10] ⁴ [12] ⁴ [14] ⁴
S_{24}	[4][8][10][12][14]	[4][6][8][10] ² [12][14] ²	S_{57}	[2][4][6] ² [8] ² [10] ³ [12] ³ [14] ³	[2][4] ² [6] ³ [8] ⁴ [10] ⁴ [12] ⁵ [14] ⁵
S_{25}	[5][7][9][11][13][15]	[3][5][7][9] ² [11] ² [13] ² [15]	S_{58}	[3][5] ² [7] ³ [9] ³ [11] ³ [13] ⁴ [15] ²	[1][3] ² [5] ³ [7] ⁴ [9] ⁵ [11] ⁶ [13] ⁶ [15] ³
S_{26}	[2][6][8][10][12] ² [14]	[2][6] ² [8] ² [10][12] ³ [14] ²	S_{66}	[1][3][5][7] ² [9] ² [11] ³ [13] ³ [15]	[1][3][5] ² [7] ⁴ [9] ³ [11] ⁴ [13] ⁵ [15] ²
S_{27}	[4][6][8][10] ² [12][14] ²	[4] ² [6][8] ² [10] ³ [12] ² [14] ³	S_{67}	[3][5] ² [7] ² [9] ³ [11] ³ [13] ³ [15] ²	[3] ² [5] ³ [7] ³ [9] ⁵ [11] ⁵ [13] ⁵ [15] ³
S_{28}	[3][5][7][9] ² [11] ² [13] ² [15]	[3][5] ² [7] ² [9] ³ [11] ³ [13] ³ [15] ²	S_{68}	[2][4] ² [6] ² [8] ³ [10] ⁴ [12] ⁴ [14] ⁴	[2][4] ³ [6] ⁴ [8] ⁵ [10] ⁶ [12] ⁶ [14] ⁷
S_{33}	[1][3][9][11] ² [13]	[5][7] ² [9][11][13] ² [15]	S_{77}	[1][3][5] ² [7] ³ [9] ³ [11] ⁴ [13] ⁴ [15] ²	[1][3] ² [5] ³ [7] ⁵ [9] ⁵ [11] ⁶ [13] ⁷ [15] ³
S_{34}	[5][7][9][11][13][15]	[3][5][7][9] ² [11] ² [13] ² [15]	S_{78}	[2][4] ² [6] ³ [8] ⁴ [10] ⁴ [12] ⁵ [14] ⁵	[2] ² [4] ³ [6] ⁵ [8] ⁶ [10] ⁷ [12] ⁸ [14] ⁸
S_{35}	[2][4][8][10] ² [12] ² [14]	[4][6] ² [8] ² [10] ² [12] ² [14] ³	S_{88}	[1][3] ² [5] ³ [7] ⁴ [9] ⁵ [11] ⁶ [13] ⁶ [15] ³	[1][3] ³ [5] ⁵ [7] ⁷ [9] ⁸ [11] ⁹ [13] ¹⁰ [15] ⁵

$F_{-p} = F_p^{-1}$, $F_0 = F_{30} = 1$, $F_{p+60} = F_p$, we can express every S -matrix element as a product of each F_p ($p = 1, \dots, 15$) with non-negative integer power $n_{ab}(p)$, $S_{ab} = \prod_{p=1}^{15} F_p^{n_{ab}(p)}$. Therefore, the (R–L) scatterings S_{ab} are essentially encoded in these exponents $n_{ab}(p)$. We find all possible solutions n_{ab} from the bootstrap equations along the following three steps.

(1) *Fix S_{11} .* The self-fusion $A_1 A_1 \rightarrow A_1$ gives the first bootstrap equation

$$S_{11}(\theta) = S_{11}\left(\theta + \frac{i\pi}{3}\right) S_{11}\left(\theta - \frac{i\pi}{3}\right). \quad (2)$$

Each solution of this provides a seed to construct all other amplitudes. The saturation bound below limits the seeds to at most four F_p blocks. The new solutions already appear at two blocks: after full directed propagation, pole-free positivity, and the saturation bound, the surviving two-block seeds are the minimal $F_1 F_{11}$ and the new golden $F_7 F_{13}$, while the saturated solution is the entrywise square $(F_1 F_{11})^2$. The diagonal completion requires no search: its R–L amplitudes are the inverses of the massive E_8 amplitudes, $S_{ab}^{\text{diag}} = (S_{ab}^{E_8})^{-1}$, which are pole-free in the physical strip and solve the same fusing equations, giving the seed $F_2 F_{10} F_{12}$.

(2) *Generate all amplitudes from S_{11} .* Each heavier particle is a bound state reached by an equal-mass fusion $A_a A_a \rightarrow A_c$, realized as a shift with the fusion angle \bar{u}_{ac}^a ; $A_1 A_1 \rightarrow A_{2,3}$ with $m = 6, 1$; $A_2 A_2 \rightarrow A_{4,5,6}$ with $m = 7, 4, 1$; $A_3 A_3 \rightarrow A_7$ with $m = 2$; and $A_4 A_4 \rightarrow A_8$ with $m = 1$ (the complete fusion angle table is in the SM [12]). The complete minimal and golden tables obtained from this procedure are listed in TABLE I; the saturated table is the entrywise square of the minimal one.

(3) *Consistency* There remain many bootstrap equa-

tions

$$S_{dc}(\theta) = S_{da}(\theta + i\bar{u}_{ac}^b) S_{db}(\theta - i\bar{u}_{bc}^a), \quad (3)$$

with the generic fusion angles \bar{u}_{ac}^b . These overdetermined equations provide a strict consistency check: all 1792 directed fusing identities hold as exact integer-vector identities for each completion in Table I. The resulting S-matrices are written as

$$S_{ab}(\theta) = \prod_{p=1}^{15} F_p(\theta)^{n_{ab}(p)}, \quad (4)$$

with integer block exponents $n_{ab}(p)$ specifying the multiplicity of each elementary CDD block F_p .

UV completeness requires the integrated R–L kernel $\hat{k}_{ab} = \sum_p n_{ab}(p)$ to satisfy $\hat{k}_{ab} \leq (2M)_{ab}$, with $M = (2\mathbb{I} - G_{E_8})^{-1}$, the inverse E_8 Cartan matrix where G_{E_8} is the mass-ordered adjacency matrix [1]. Seeds violating the saturation bound, $\hat{k}_{11} > 4$, produce a Hagedorn divergence in the UV limit. A simple check over all possible S_{11} against the saturation bounds leaves exactly four pole-free UV completions, with $c_{UV} = 21/22, 25/14, 15/2, 31/2$ for the minimal, golden, diagonal, and saturated seeds (SM).

III. TBA AND THE Y-SYSTEM

A. Inversion relations and the universal kernel

In the standard derivation of the TBA equations, the pseudo-energies of the R-particles couple to those of the L-particles. The Fourier transform of the R–L kernel

matrix, whose elements are the logarithmic derivatives of the S_{ab} , can be obtained by (4)

$$\Psi(q) = \sum_{p=1}^{15} n(p) (q^{15-p} + q^{p-15}), \quad q = e^{\pi\omega/30} \quad (5)$$

where each factor $q^{15-p} + q^{p-15}$ comes from the Fourier transform of $F_p(\theta)$.

The E_8 symmetry appears in universal TBA equations where kernels connecting the R and L pseudo-energies are given by $[(q + q^{-1})\mathbb{I} - G_{E_8}] \Psi(q)$. This can be rewritten with Chebyshev polynomials T_n

$$2 \sum_{p=1}^{15} n(p) (2T_1(x)\mathbb{I} - G_{E_8}) T_{15-p}(x), \quad x = \frac{q + q^{-1}}{2} \quad (6)$$

where G_{E_8} is the adjacency matrix of the E_8 . It turns out that the exponent matrices $n(p)$ given in TABLE I satisfy interesting recursion relations

$$(1 + \delta_{p,14})n(p+1) + n(p-1) = G_{E_8}n(p), \quad (7)$$

where $p = 1, \dots, 15$ with $n(0) = n(16) \equiv 0$ are implied. These relations and Chebyshev identity $2T_1(x)T_n(x) = T_{n+1}(x) + T_{n-1}(x)$ make the intermediate Chebyshev coefficients all cancel, leaving only the boundary term,

$$[(q + q^{-1})\mathbb{I} - G_{E_8}] \Psi(q) = (q^{15} + q^{-15})\mathbb{N}, \quad (8)$$

where we use $\mathbb{N} = n(1)$ for simplicity. For the minimal S -matrix in TABLE I, the [1] factor appears only in S_{aa} , hence, $\mathbb{N} = n(1) = \mathbb{I}_8$. For the golden solution, the exponent matrix can be written as

$$\mathbb{N} = \begin{pmatrix} 0 & 1 & 0 & 0 & 0 & 0 & 0 & 0 \\ 1 & 1 & 0 & 0 & 0 & 0 & 0 & 0 \\ 0 & 0 & 0 & 0 & 0 & 1 & 0 & 0 \\ 0 & 0 & 0 & 0 & 0 & 0 & 1 & 0 \\ 0 & 0 & 0 & 0 & 0 & 0 & 0 & 1 \\ 0 & 0 & 1 & 0 & 0 & 1 & 0 & 0 \\ 0 & 0 & 0 & 1 & 0 & 0 & 1 & 0 \\ 0 & 0 & 0 & 0 & 1 & 0 & 0 & 1 \end{pmatrix} = A_{\text{Fib}}^{\oplus 4}, \quad A_{\text{Fib}} = \begin{pmatrix} 0 & 1 \\ 1 & 1 \end{pmatrix}. \quad (9)$$

We call this structure golden/Fibonacci because the golden kernel obeys

$$\mathbb{N}^2 = \mathbb{N} + \mathbb{I}, \quad (10)$$

where the four pairs, connected by \mathbb{N}

$$\{1, 2\}, \quad \{3, 6\}, \quad \{4, 7\}, \quad \{5, 8\},$$

are precisely the golden doublets of the mass spectrum,

$$\frac{m_2}{m_1} = \frac{m_6}{m_3} = \frac{m_7}{m_4} = \frac{m_8}{m_5} = \varphi.$$

Thus the golden ratio visible in the massive E_8 spectrum reappears here as a kernel-level Fibonacci structure.

The Y -systems for each UV-complete solution can be derived as follows:

$$Y_a^R(\theta + \frac{i\pi}{30}) Y_a^R(\theta - \frac{i\pi}{30}) = \prod_{b=1}^8 \frac{(1 + Y_b^R)^{(G_{E_8})_{ab}}}{(1 + 1/Y_b^L)^{\mathbb{N}_{ab}}}, \quad (11)$$

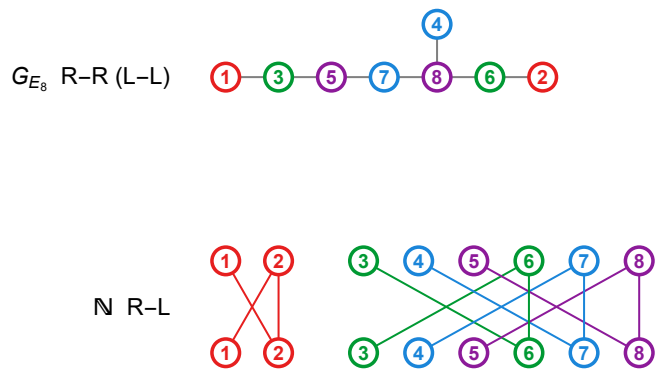


FIG. 1. Top: the mass-ordered E_8 adjacency graph, with node labels denoting the particle mass ordering. Bottom: the golden R-L coupling graph in the same mass-ordered basis. The colored links indicate the four Fibonacci blocks associated with the golden doublets.

where the adjacency graphs connecting the R- and L-nodes are plotted in FIG.1. It is remarkable that all the \mathbb{N} adjacency matrices for the UV complete theories can be written as a universal form

$$\mathbb{N}^{[n]} = 2T_n(G_{E_8}/2), \quad n = 10, 6, 1, 0. \quad (12)$$

Furthermore, only the above $T_n(G_{E_8}/2)$ have non-negative matrix elements among all positive divisors n of 30. This is consistent with the UV completeness since the Y -systems become singular if some \mathbb{N}_{ab} become negative.

B. UV central charge and relevant field from exact periodicity

In the UV plateau the constant TBA solution gives, through the Rogers-dilogarithm sum, $c_{\text{UV}} = 25/14$ for the golden flow. The dimension of the UV relevant field can be read directly from the periodicity of the Y -system (11). For the golden completion the exact period analysis gives $P_{\text{TBA}} = 35$, and therefore

$$\Delta_{\text{rel}} = 2 - \frac{60}{P_{\text{TBA}}} = \frac{2}{7}. \quad (13)$$

The same analysis gives $\Delta_{\text{rel}} = 2/11$ and 1 for the minimal and diagonal completions ($P_{\text{TBA}} = 33, 60$), while the saturated case lies outside the finite ADE periodic family and is treated as the $P_{\text{TBA}} = \infty$ marginal endpoint ($\Delta_{\text{rel}} = 2$). The four completions are collected in TABLE II.

C. Numerical golden flow

Solving the golden TBA numerically, we find that the effective central charge rises monotonically from $c_{\text{IR}} =$

completion	\mathbb{N}	n	c_{UV}	Δ_{rel}
minimal	\mathbb{I}	10	21/22	2/11
golden	$A_{Fib}^{\oplus 4}$	6	25/14	2/7
diagonal	G_{E_8}	1	15/2	1
saturated	$2\mathbb{I}$	0	31/2	2

TABLE II. The four UV completions: constant kernel $\mathbb{N} = 2T_n(G_{E_8}/2)$, UV central charge, and relevant dimension $\Delta_{rel} = 2 - 60/P_{TBA}$ with $P_{TBA} = 33, 35, 60, \infty$. The saturated entry is marginal.

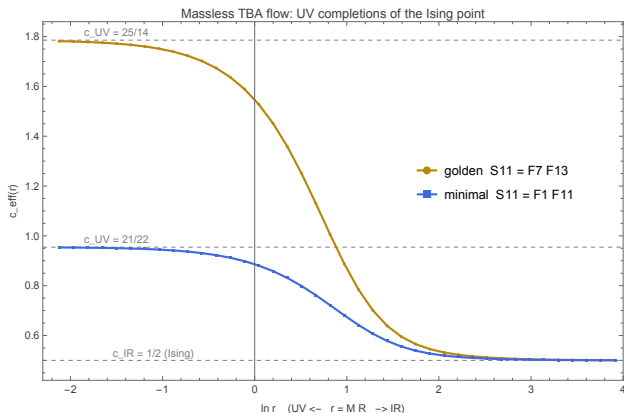


FIG. 2. Effective central charge $c_{eff}(r)$ from the numerical TBA. The minimal curve is included as a reference, while the golden flow generated by $F_7 F_{13}$ rises from the infrared Ising value $1/2$ to the new ultraviolet plateau $25/14$.

$1/2$ to the UV plateau $25/14$ for the golden and $21/22$ for the minimal flows (Fig. 2). The golden L -functions are bell-shaped and mass-ordered (SM, Fig. S1), as expected for a relevant, minimal-type massless flow.

D. Identification of the golden UV CFT

The UV CFT for the minimal flow is well-known to be a coset CFT with the relevant coset field

$$\frac{E_{8,1} \times E_{8,2}}{E_{8,3}} + \lambda \Phi_{rel}, \quad \Phi_{rel} = \left[\frac{(1; \circ) \otimes (2; \circ)}{(3; Adj)} \right], \quad (14)$$

where $(k; \circ)$ denotes a singlet representation of the E_8 WZW CFT with a level k .

From the UV conformal data for the golden flow

$$(c_{UV}, \Delta_{rel}) = \left(\frac{25}{14}, \frac{2}{7} \right), \quad (15)$$

we identify it as another coset CFT

$$\frac{su(2)_5 \times su(2)_5}{su(2)_{10}}, \quad c = \frac{25}{14}. \quad (16)$$

The central charge alone is not claimed to determine the UV theory uniquely. We therefore check whether the relevant field with $\Delta = 2/7$ can exist in the field content

of the coset CFT. In terms of the $su(2)$ representations, the highest weight states of the coset can be written as $(\ell_1, \ell_2; \ell_3)$ with $0 \leq \ell_{1,2} \leq 5$, $0 \leq \ell_3 \leq 10$, $\ell_1 + \ell_2 + \ell_3 \in 2\mathbb{Z}$ and the field identification

$$(\ell_1, \ell_2; \ell_3) \sim (5 - \ell_1, 5 - \ell_2; 10 - \ell_3), \quad (17)$$

the conformal weight (mod 1) is

$$h = \frac{\ell_1(\ell_1 + 2)}{28} + \frac{\ell_2(\ell_2 + 2)}{28} - \frac{\ell_3(\ell_3 + 2)}{48}. \quad (18)$$

We find that

$$(1, 3; 4) \sim (3, 1; 4) \sim (2, 4; 6) \sim (4, 2; 6) \quad (19)$$

give the primary field with $\Delta = 2h = 2/7$.

Another interesting point is known in mathematical literature that the period of the coupled Y -systems is given by sum of the individual periods (see [11] and references therein). Accordingly, the period of the golden Y -system can be interpreted as $P_{TBA} = 5 + 30 = h_{A_4} + h_{E_8}$, a sum of two dual Coxeter numbers. Along with a level-rank duality between $su(2)_5$ and $su(5)_2$, the period and the UV diagonal $su(2)_5$ coset are consistent.

IV. DISCUSSION

The four sets of the R–L S -matrices generate the UV-complete integrable massless flows from the Ising CFT deformed by the higher- $T\bar{T}$ -type deformations. The new golden flow, which had not even been conjectured before, moves toward the UV CFT along a relevant $\Delta_{rel} = 2/7$ field direction. The corresponding UV CFT is identified with a diagonal $su(2)_5$ coset which flows from $c = 25/14$ to $c = 1/2$. The golden ratio visible in the E_8 mass spectrum reappears in the UV completion as a kernel-level Fibonacci structure, $N_{Fib} = A_{Fib}^{\oplus 4}$ and $N_{Fib}^2 = N_{Fib} + I$.

We have also found that the four UV complete RG flows have an interesting common feature, namely, all the R–L adjacency matrices are given by (12) along with the TBA periods given by a universal formula $P_{TBA} = 30 + 30/n$ for $n = 1, 6, 10$, with the saturated case $n = 0$ understood as the marginal $P_{TBA} = \infty$ endpoint.

In conclusion, the beautiful E_8 structure discovered in the 2D Ising CFT with the magnetic deformation [4] persists even in the UV completion generated by the same theory deformed by higher irrelevant deformations through the UV-complete massless flows constructed here.

ACKNOWLEDGMENTS

This work is supported by the National Research Foundation of Korea (NRF) through grants RS-2026-25472596 (CA) and RS-2025-25414114 (MK).

Corresponding Authors:

†ahn@ewha.ac.kr, ‡minkyookim@snu.ac.kr.

-
- [1] C. Ahn and A. LeClair, “On the classification of UV completions of integrable $T\bar{T}$ deformations of CFT,” *JHEP* **08** (2022), 179 [arXiv:2205.10905 [hep-th]].
- [2] F. A. Smirnov and A. B. Zamolodchikov, “On space of integrable quantum field theories,” *Nucl. Phys. B* **915** (2017), 363-383 [arXiv:1608.05499 [hep-th]].
- [3] A. Cavaglià, S. Negro, I. M. Szécsényi and R. Tateo, “ $T\bar{T}$ -deformed 2D Quantum Field Theories,” *JHEP* **10** (2016), 112 [arXiv:1608.05534 [hep-th]].
- [4] A. B. Zamolodchikov, “Integrals of Motion and S Matrix of the (Scaled) $T=\bar{T}(c)$ Ising Model with Magnetic Field,” *Int. J. Mod. Phys. A* **4** (1989), 4235.
- [5] R. Coldea, D. A. Tennant, E. M. Wheeler, E. Wawrzynska, D. Prabhakaran, M. Telling, K. Habicht, P. Smeibidl and K. Kiefer, “Quantum Criticality in an Ising Chain: Experimental Evidence for Emergent $E(8)$ Symmetry,” *Science* **327** (2010), 177-180 [arXiv:1103.3694 [cond-mat.str-el]].
- [6] A. B. Zamolodchikov, “From Tricritical Ising to Critical Ising By Thermodynamic Bethe ansatz,” *Nucl. Phys.* **B358** (1991), 524.
- [7] C. Ahn, C. Kim, C. Rim, and A.B. Zamolodchikov, “RG flows from super-Liouville theory to critical Ising model,” *Phys. Lett.* **B541** (2002), 194.
- [8] A. LeClair, “Deformation of the Ising model and its ultraviolet completion,” *J. Stat. Mech.* **2111** (2021), 113104 [arXiv:2107.02230].
- [9] F. Ravanini, “Thermodynamic Bethe Ansatz for $G_k \otimes G_\ell/G_{k+\ell}$ coset models perturbed by their $\phi_{1,1,Adj}$ operator,” *Phys. Lett.* **B282** (1992) 73, [arXiv:hep-th/9202020].
- [10] C. Ahn, “Massless S-matrix bootstraps and RG flows,” *JHEP* **12** (2025), 103 [arXiv:2509.20740 [hep-th]].
- [11] P. Galashin and P. Pylyavskyy, “The classification of Zamolodchikov periodic quivers,” *Amer. J. Math.* **141**, 447 (2019), [arXiv:1603.03942 [math.CO]].
- [12] See Supplemental Material below for Saturation bounds, Inversion relations, the numerical TBA results, and the coset branching spectrum.

Supplemental Material (SM)

UV completion of 2D Ising CFT: a golden E_8 massless S -matrix

Changrim Ahn and Minkyoo Kim

S1. SATURATION BOUNDS FOR E_8 BOOTSTRAPS

The mass-ordered E_8 spectrum, given by the components of the Perron-Frobenius eigenvector, is

$$\begin{aligned}
 m_1 &= 1, & m_2 &= 2 \cos \frac{\pi}{5}, & m_3 &= 2 \cos \frac{\pi}{30}, \\
 m_4 &= 4 \cos \frac{\pi}{5} \cos \frac{7\pi}{30}, & m_5 &= 4 \cos \frac{\pi}{5} \cos \frac{2\pi}{15}, \\
 m_6 &= 4 \cos \frac{\pi}{5} \cos \frac{\pi}{30}, & m_7 &= 8 \cos^2 \frac{\pi}{5} \cos \frac{7\pi}{30}, \\
 m_8 &= 8 \cos^2 \frac{\pi}{5} \cos \frac{2\pi}{15}.
 \end{aligned} \tag{S1}$$

The mass-ordered adjacency matrix G_{E_8} and the inverse Cartan matrix are given by

$$G_{E_8} = \begin{pmatrix} 0 & 0 & 1 & 0 & 0 & 0 & 0 & 0 \\ 0 & 0 & 0 & 0 & 0 & 1 & 0 & 0 \\ 1 & 0 & 0 & 0 & 1 & 0 & 0 & 0 \\ 0 & 0 & 0 & 0 & 0 & 0 & 0 & 1 \\ 0 & 0 & 1 & 0 & 0 & 0 & 1 & 0 \\ 0 & 1 & 0 & 0 & 0 & 0 & 0 & 1 \\ 0 & 0 & 0 & 0 & 1 & 0 & 0 & 1 \\ 0 & 0 & 0 & 1 & 0 & 1 & 1 & 0 \end{pmatrix}, \quad M = \begin{pmatrix} 2 & 2 & 3 & 3 & 4 & 4 & 5 & 6 \\ 2 & 4 & 4 & 5 & 6 & 7 & 8 & 10 \\ 3 & 4 & 6 & 6 & 8 & 8 & 10 & 12 \\ 3 & 5 & 6 & 8 & 9 & 10 & 12 & 15 \\ 4 & 6 & 8 & 9 & 12 & 12 & 15 & 18 \\ 4 & 7 & 8 & 10 & 12 & 14 & 16 & 20 \\ 5 & 8 & 10 & 12 & 15 & 16 & 20 & 24 \\ 6 & 10 & 12 & 15 & 18 & 20 & 24 & 30 \end{pmatrix}. \tag{S2}$$

The fusion angles that generate the bootstrap equations are listed in TABLE S1.

$\{a, b, c\}$	u_{ab}^c	u_{ac}^b	u_{bc}^a	$\{a, b, c\}$	u_{ab}^c	u_{ac}^b	u_{bc}^a	$\{a, b, c\}$	u_{ab}^c	u_{ac}^b	u_{bc}^a	$\{a, b, c\}$	u_{ab}^c	u_{ac}^b	u_{bc}^a
$\{1, 1, 1\}$	20	20	20	$\{1, 7, 8\}$	5	26	29	$\{3, 3, 3\}$	20	20	20	$\{4, 5, 5\}$	19	19	22
$\{1, 1, 2\}$	12	24	24	$\{1, 8, 8\}$	16	16	28	$\{3, 3, 5\}$	14	23	23	$\{4, 5, 8\}$	9	25	26
$\{1, 1, 3\}$	2	29	29	$\{2, 2, 2\}$	20	20	20	$\{3, 3, 6\}$	12	24	24	$\{4, 7, 7\}$	18	18	24
$\{1, 2, 2\}$	18	18	24	$\{2, 2, 4\}$	14	23	23	$\{3, 3, 7\}$	4	28	28	$\{4, 7, 8\}$	14	21	25
$\{1, 2, 3\}$	14	21	25	$\{2, 2, 5\}$	8	26	26	$\{3, 4, 5\}$	16	21	23	$\{5, 5, 5\}$	20	20	20
$\{1, 2, 4\}$	8	25	27	$\{2, 2, 6\}$	2	29	29	$\{3, 5, 7\}$	13	22	25	$\{5, 5, 8\}$	12	24	24
$\{1, 3, 4\}$	13	21	26	$\{2, 3, 3\}$	19	19	22	$\{3, 5, 8\}$	5	27	28	$\{5, 6, 7\}$	17	21	22
$\{1, 3, 5\}$	3	28	29	$\{2, 3, 6\}$	9	25	26	$\{3, 6, 6\}$	18	18	24	$\{5, 8, 8\}$	18	18	24
$\{1, 4, 4\}$	17	17	26	$\{2, 4, 7\}$	5	27	28	$\{3, 6, 8\}$	8	25	27	$\{6, 6, 6\}$	20	20	20
$\{1, 4, 5\}$	11	22	27	$\{2, 5, 6\}$	16	19	25	$\{3, 8, 8\}$	17	17	26	$\{6, 6, 8\}$	14	23	23
$\{1, 4, 6\}$	7	25	28	$\{2, 6, 7\}$	13	21	26	$\{4, 4, 4\}$	20	20	20	$\{6, 7, 8\}$	16	21	23
$\{1, 5, 6\}$	14	19	27	$\{2, 6, 8\}$	3	28	29	$\{4, 4, 6\}$	16	22	22	$\{7, 7, 7\}$	20	20	20
$\{1, 5, 7\}$	4	27	29	$\{2, 7, 7\}$	17	17	26	$\{4, 4, 7\}$	12	24	24	$\{7, 8, 8\}$	19	19	22
$\{1, 6, 7\}$	9	23	28	$\{2, 7, 8\}$	11	22	27	$\{4, 4, 8\}$	2	29	29	$\{8, 8, 8\}$	20	20	20

TABLE S1. The 56 E_8 fusion triples and their external angles u_{ab}^c (units of $\pi/30$), obeying $u_{ab}^c + u_{ac}^b + u_{bc}^a = 60$.

All S_{1a} can satisfy the seed condition (2) since a is just a spectator. Note that candidates for new S_{11} that satisfy the first saturation bound $\widehat{k}_{11} \leq 4$ (at most four F_p factors) are

$$S_{11}^{\min}, S_{11}^{\text{gold}}, S_{11}^{\min} \cdot S_{11}^{\text{gold}}, S_{13}^{\min}, S_{14}^{\min}, S_{15}^{\min}, S_{16}^{\min}, S_{12}^{\text{gold}}, S_{13}^{\text{gold}}, (S_{11}^{\min})^2, (S_{11}^{\text{gold}})^2. \tag{S3}$$

Only the following four of these satisfy the second saturation bound $\widehat{k}_{12} \leq 4$ for S_{12}^{new} obtained from S_{11}^{new} with the fusion angle u_{12}^1

$$S_{11}^{\min}, S_{11}^{\text{gold}}, S_{13}^{\min}, (S_{11}^{\min})^2. \tag{S4}$$

Furthermore, each of these satisfies $\widehat{k}_{ab} \leq 2M_{ab}$ for all $a, b = 1, \dots, 8$. These are the minimal, golden, diagonal, and saturated seeds, summarized in TABLE S2.

completion	seed S_{11}	\mathbb{N}	c_{UV}
minimal	[1][11]	\mathbb{I}	21/22
golden	[7][13]	$A_{\text{Fib}}^{\oplus 4}$	25/14
diagonal	[2][10][12]	G_{E_8}	15/2
saturated	$([1][11])^2$	$2\mathbb{I}$	31/2

TABLE S2. The four UV-complete seeds selected by the saturation criterion; $[p] \equiv F_p$ as in Table I.

S2. INVERSION RELATIONS AND R-L ADJACENCY MATRICES

Using the Chebyshev identity $2T_1(x)T_n(x) = T_{n+1}(x) + T_{|n-1|}(x)$ on (6), we can rewrite it as

$$2T_{15}(x)n(1) + 2 \sum_{p=1}^{15} [(1 + \delta_{p,14})n(p+1) + n(p-1) - G_{E_8}n(p)] T_{15-p}(x), \quad (\text{S5})$$

where the second sum vanishes due to the relations satisfied by the exponent matrices

$$(1 + \delta_{p,14})n(p+1) + n(p-1) = G_{E_8}n(p). \quad (\text{S6})$$

This leads to

$$[(q + q^{-1})\mathbb{I} - G_{E_8}]\Psi(q) = (q^{15} + q^{-15})\mathbb{N}, \quad n(1) = \mathbb{N}. \quad (\text{S7})$$

S3. NUMERICAL TBA/Y-SYSTEMS

From the inversion relations, we can derive the universal TBA equations as follows:

$$\epsilon_a^R(\theta) = r\nu_a^R + \varphi \star \sum_{b=1}^8 [(G_{E_8})_{ab} (\mathcal{L}_b^R - \nu_b^R) - \mathbb{N}_{ab} L_b^L](\theta), \quad a = 1, \dots, 8, \quad (\text{S8})$$

and another set of equations by exchanging $R \leftrightarrow L$. We use the standard convolution \star and $\nu_a^R = m_a e^\theta, \nu_a^L = m_a e^{-\theta}$. The universal kernel φ and L -functions are defined by

$$\varphi = \frac{1}{2 \cosh \theta}, \quad \mathcal{L}_a^{R/L} = \log [1 + e^{\epsilon_a^{R/L}(\theta)}], \quad L_a^{R/L}(\theta) = \log [1 + e^{-\epsilon_a^{R/L}(\theta)}], \quad \epsilon_a^L(\theta) = \epsilon_a^R(-\theta). \quad (\text{S9})$$

In terms of these, the scaling energy of the ground state and the effective central charge are given by

$$E(r) = \frac{\pi c_{\text{eff}}(r)}{6r} = -\frac{1}{2\pi} \sum_{a=1}^8 \int_{-\infty}^{\infty} d\theta [\nu_a^R(\theta) L_a^R(\theta) + \nu_a^L(\theta) L_a^L(\theta)]. \quad (\text{S10})$$

A standard iteration algorithm for the TBA equations is applied to generate the RG flows as a function of the scale r , as shown in FIG.2. We can also obtain the plateau values by plotting the L -functions in the deep UV as shown in FIG.S1. For the golden solution, the plateau values of Y_a^R are given by

$$Y_a^R \simeq (2.5717, 2.9608, 7.8475, 8.2959, 15.287, 17.370, 33.589, 69.871), \quad (\text{S11})$$

giving $c_{UV} = 25/14$ in terms of the Rogers dilogarithm sum. The Y -system can also be used to find the half-period, which is related to the dimension of the perturbing operator. For the golden case, $P_{\text{TBA}} = 35$, which corresponds to $\Delta_{\text{rel}} = 2/7$.

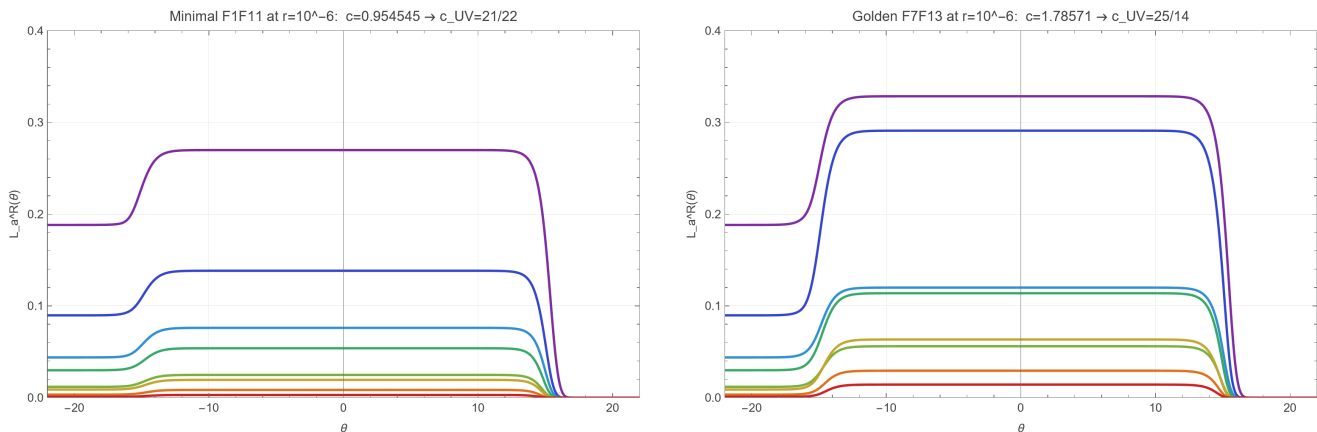


FIG. S1. L -functions $L_a^R(\theta)$ for minimal and golden completions at $r = 10^{-6}$. In each panel the eight curves are ordered by mass and colored from purple (lightest, top plateau) to red (heaviest, bottom): L_1^R ($m_1=1.000$), L_2^R ($m_2=1.618$), L_3^R ($m_3=1.989$), L_4^R ($m_4=2.405$), L_5^R ($m_5=2.956$), L_6^R ($m_6=3.218$), L_7^R ($m_7=3.891$), L_8^R ($m_8=4.783$), in units $m_1 = 1$. The wide flat plateau is the UV conformal fixed point, where the dilogarithm sum of the plateau values reproduces c_{UV} ; the curves drop to the trivial vacuum for $\theta \gtrsim \log(2/r)$.

S4. AFFINE-BRANCHING SPECTRUM OF THE DIAGONAL $su(2)_5$ COSET

The diagonal $su(2)_5$ coset of Eq. (16) has primaries $(\ell_1, \ell_2; \ell_3)$ with

$$0 \leq \ell_1, \ell_2 \leq 5, \quad 0 \leq \ell_3 \leq 10, \quad \ell_1 + \ell_2 + \ell_3 \in 2\mathbb{Z}, \quad (\text{S12})$$

modulo the field identification (17).

The physical conformal weight is computed from affine branching functions, defined by characters $\widehat{\chi}_\ell^{(k)}$ of the $su(2)_k$ WZW model as follows:

$$\widehat{\chi}_{\ell_1}^{(5)}(q, z) \widehat{\chi}_{\ell_2}^{(5)}(q, z) = \sum_{\ell_3=0}^{10} b_{\ell_1 \ell_2}^{\ell_3}(q) \widehat{\chi}_{\ell_3}^{(10)}(q, z). \quad (\text{S13})$$

From this, the holomorphic dimensions of the primary states of the coset CFT are given by

$$h_{\text{phys}} = h_{\ell_1}^{(5)} + h_{\ell_2}^{(5)} - h_{\ell_3}^{(10)} + n_{\text{min}}, \quad h_\ell^{(k)} = \frac{\ell(\ell+2)}{4(k+2)}, \quad (\text{S14})$$

where n_{min} should be chosen to make the dimensions non-negative.

From this formula, we obtain low-lying dimensions as shown in Table S3. The $h = 1/7$ entry of Table S3 is found at

$$(1, 3; 4) \sim (3, 1; 4) \sim (2, 4; 6) \sim (4, 2; 6) \quad (\text{S15})$$

as given in Eq. (19) of the main text.

h_{phys}	decimal	$(\ell_1, \ell_2; \ell_3)$	h_{phys}	decimal	$(\ell_1, \ell_2; \ell_3)$
0	0.00000	(0, 0; 0)	25/112	0.22321	(0, 3; 3)
5/112	0.04464	(0, 1; 1)	79/336	0.23512	(1, 4; 5)
1/21	0.04762	(1, 1; 2)	37/112	0.33036	(1, 2; 1)
1/14	0.07143	(2, 2; 4)	5/14	0.35714	(0, 4; 4)
9/112	0.08036	(1, 2; 3)	17/42	0.40476	(2, 2; 2)
31/336	0.09226	(2, 3; 5)	10/21	0.47619	(1, 3; 2)
5/42	0.11905	(0, 2; 2)	57/112	0.50893	(2, 3; 3)
1/7	0.14286	(1, 3; 4)	25/48	0.52083	(0, 5; 5)
3/14	0.21429	(1, 1; 0)	4/7	0.57143	(2, 2; 0)

TABLE S3. Low-lying genuine conformal weights of the golden coset. The $h = 1/7$ entry is the perturbing orbit selected by the Y -system.